Journal of Hematology & Oncology

RESEARCH

Open Access

UVI5008: the first reversible, non-covalent Bruton's tyrosine kinase epi-inhibitor for B-cell malignancies

Carmela Dell'Aversana[1,2,3*†], G. Sgueglia[1†], C. Massaro[1], U. Perricone[4], F. Sarno[1,5], W. L. Megchelenbrink[1], M. Conte[1], V. Carafa[1], A. Campanella[6,7], M. Frenquelli[6], J. Bordini[6], P. Ghia[6,7], V. B. Petrizzi[8], R. Alvarez[9], D. Nappi[10], F. Chiurazzi[10], F. P. Tambaro[11], W. G. Wierda[12], A. R. de Lera[9] and Lucia Altucci[1,13,14*]

Abstract

Background Chronic lymphocytic leukemia (CLL) can still be a therapeutic challenge; notwithstanding substantial progress in therapeutic approaches with small molecule inhibitors, the emergence of inhibitor resistance and suboptimal long-term outcomes highlight the persistent need for novel, more effective treatment strategies, especially targeting resistance.

Patients and methods Kinase activity screening was performed on UVI5008, followed by computational study. The findings were validated through a comprehensive set of in vitro and ex vivo assays, including enzymatic, cellular, transcriptional, genetic, epigenetic, and genomic assays, on primary CLL patient-derived peripheral blood mononuclear cells and cell lines, as well as through in vivo studies using genetically engineered mouse models.

Results We identified a novel tyrosine kinase inhibitory activity of UVI5008, currently the only known epigenetic modulator (epi-inhibitor) that directly targets Bruton's tyrosine kinase (BTK), affecting both BTK expression and enzymatic function. Our comprehensive analysis, combining in silico, ex vivo, and in vivo approaches, revealed that UVI5008 effectively inhibits both wild-type BTK and the C481S mutated BTK isoform, commonly associated with BTK-inhibitor resistance in CLL. Treatment with UVI5008 in B-cell lymphoma and leukemia disorders led to a substantial increase in cellular apoptosis, accompanied by a notable reduction in phosphorylation and BTK protein levels, as well as attenuation of downstream signaling, thus demonstrating superior efficacy compared to ibrutinib. Ex vivo treatment of patient-derived CLL samples and in vivo murine models corroborated these results, further supporting the potential of UVI5008 as a promising therapeutic agent.

Conclusion UVI5008 represents a promising pharmacological alternative to current BTK inhibitors. As the first-in-class, non-covalent, reversible, BTK inhibitor and epi-inhibitor of expression. UV15008 demonstrates potent in vitro

†Carmela Dell'Aversana and G. Sgueglia contributed equally to this work.

*Correspondence:
Carmela Dell'Aversana
dellaversana@lum.it
Lucia Altucci
lucia.altucci@unicampania.it

Full list of author information is available at the end of the article

anti-tumor efficacy in relapsed/refractory CLL cells, including cases with the C481S BTK mutation and in in vivo animal studies.

Highlights

- UVI5008 is a first-in-class reversible, non-covalent enzymatic inhibitor and epi-inhibitor of expression of Bruton's tyrosine kinase (BTK).
- UVI5008 exhibits potent binding and inhibition of both wild-type BTK and the resistance-associated C481S BTK mutant.
- UVI5008 shows robust antitumor activity in B-cell lymphoma/leukemia cell lines, primary patient derived CLL cells, and in the TCL1 mouse model.
- UVI5008 has therapeutic potential in BTK-inhibitor resistant B-cell malignancies.

Keywords BTK, CLL, UVI5008, Epi-inhibitor, BTK C481S mutation

Graphical abstract

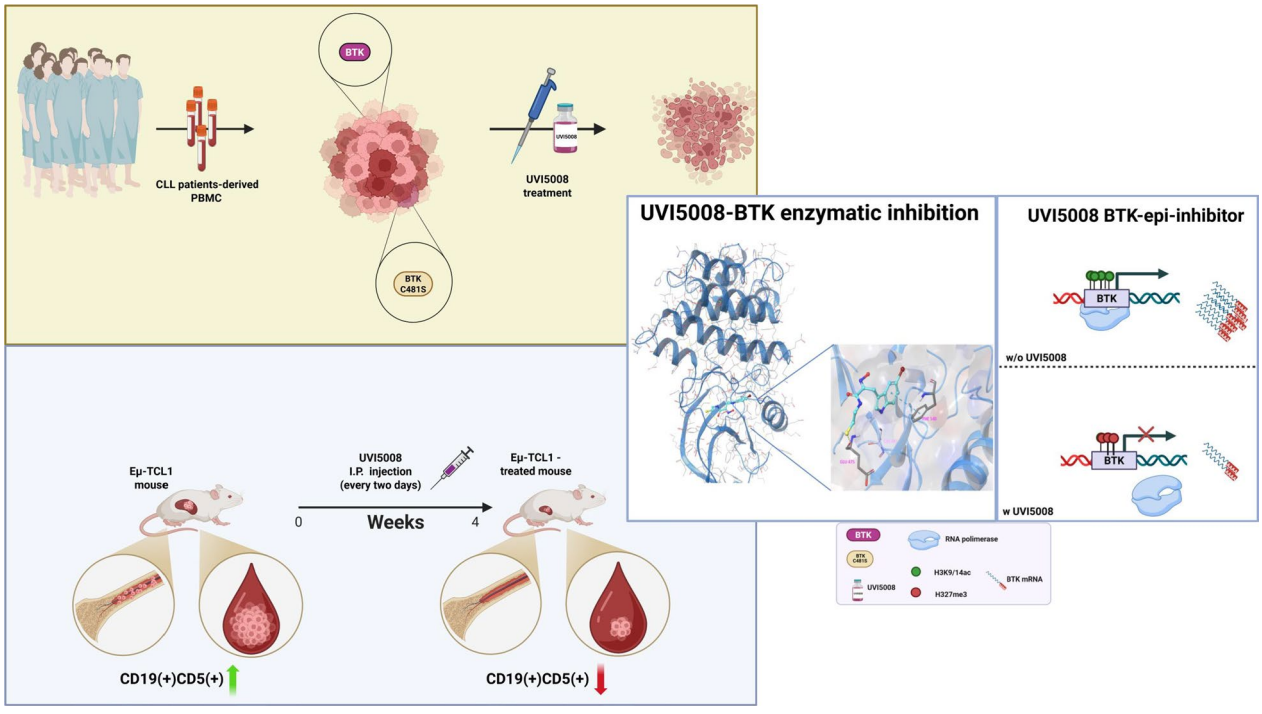

Background

Aberrant activation of kinase signaling pathways is a hallmark of B-cell malignancies. One key deregulated pathway involves heightened expression and activation of various components of the B-cell receptor (BCR) signaling cascade, particularly Bruton's tyrosine kinase (BTK) [1]. BTK plays a central role in regulating critical biological processes, including cellular proliferation, apoptosis, cytoskeletal reorganization, motility, metabolism, angiogenesis, and immune evasion in tumors [2–4]. BTK inhibitors (BTKi) have revolutionized the treatment landscape for B-cell malignancies, such as chronic lymphocytic leukemia (CLL), mantle cell lymphoma (MCL), lymphoplasmacytic lymphoma/Waldenström macroglobulinemia, and small lymphocytic lymphoma [5]. CLL is a clonal hematologic malignancy marked by the progressive accumulation of mature, but functionally impaired $CD5^+$ B-lymphocytes in peripheral blood (PB), bone marrow (BM), and lymphoid tissues [6]; it predominantly affects the elderly (diagnosed around age 70), with its progressive nature leading to significant morbidity and mortality. While CLL often presents indolently in early stages, it can evolve into a more aggressive form characterized by complications including infections, autoimmune phenomena, and organ infiltration [6].

CLL pathogenesis is associated with aberrant genetic mutations, particularly those affecting the BCR signaling pathway [7] such as mutations in *BTK* and *PLCγ2*, leading to survival and clonal expansion of malignant B-cells [1]. Despite significant therapeutic advances with covalent BTK-inhibitors (BTKi) such as ibrutinib, acalabrutinib, and zanubrutinib, agents that irreversibly bind

to the cysteine 481 residue of BTK, long-term disease control in CLL remain elusive. This is largely due to the emergence of sub-clonal resistance and ultimate relapse in a substantial proportion of patients [8–10]. Resistance is frequently associated with mutations in BTK (e.g., C481S), impairing the binding of covalent inhibitors and leading to treatment failure [9], or activating mutations in the downstream effector PLCγ2 [11]. Non-covalent reversible BTKi are active in treating CLL resistant to covalent BTKi, including in patients harboring BTK C481 mutations. Currently there is one available non-covalent BTKi, pirtobrutinib (LOXO-305; Jaypirca®). Pirtobrutinib has efficacy in patients with CLL resistant to covalent BTKi, including those carrying C481S mutations, although responses have limited durability. Pirtobrutinib is approved by the US FDA and the EU EMA for the treatment of patients with CLL or small lymphocytic lymphoma (SLL) previously exposed to a BTKi [12]. However, the need for alternative, more potent and durable therapeutic strategies remains critical, particularly for patients who develop resistance to current BTKi treatments [13].

Epigenomics of B-cell malignancies contribute to clonal evolution, relapse, and therapeutic resistance. In CLL, epigenetic deregulation is a key driver of disease progression and a promising therapeutic target [14–16].UVI5008, a structural analog of natural product psammaplin A, exhibits inhibitory activity against specific epigenetic enzymes: histone deacetylases, DNA methyltransferase 3a, and sirtuins 1 and 2 [17–19]. This unique inhibitory profile makes UVI5008 a promising candidate for anticancer therapy. The compound demonstrates broad-spectrum cytotoxicity across various human cancer cell lines, including leukemia (K562, U937), breast (MCF7), colon (HCT116), and prostate (DU145) cancer, and melanoma (A375) [20]. Mechanistically, in both in vitro and in vivo models, the antitumor efficacy of UVI5008 is further supported by activation of death receptor signaling pathways and induction of reactive oxygen species, occurring independently of canonical apoptotic mediators (e.g. TP53, BMF, TRAIL) [20]. Here, we identified and characterized a new activity of UVI5008 as a direct inhibitor of BTK, impacting both its transcriptional expression (via chromatin resetting) and enzymatic activity. This dual mechanism of action may provide a therapeutic advantage in BTKi-resistant malignancies, making UVI5008 a first-in-class enzymatic inhibitor that also exerts negative gene regulation through epigenetic modulation, a novel drug we called an "epi-inhibitor", with potential to overcome resistance-associated treatment failure.

Methods

Patients and cell lines

Mec-1 (RRID: ACC 497) and Mino (RRID: ACC 687) and K562 (RRID: CVCL_0004)cell lines were cultured in RPMI 1640 medium (EuroClone) supplemented with 10% and 20% heat-inactivated fetal bovine serum (FBS) (EuroClone, ECS5000L), respectively, 1% glutamine (MicroGem, TCL012), 1% penicillin/streptomycin (EuroClone, ECB3001D), and 0.01% amphotericin B (EuroClone, ECM0009D). Granta-519 (RRID: ACC 342) cells were cultured in DMEM (EuroClone) supplemented with 10% heat-inactivated FBS (EuroClone, ECS5000L), 1% glutamine (MicroGem, TCL012), 1% penicillin/streptomycin (EuroClone, ECB3001D), and 0.01% amphotericin B (EuroClone, ECM0009D). PB samples from CLL patients were obtained from a cohort of 52 patients (Supplementary Table 1), in accordance with ethical guidelines approved by the University of Campania "Luigi Vanvitelli" Hospital Ethics Committee (protocol n. 296) and by "Federico II" University Hospital Ethical Committee (protocol n. 347/19).

RNA sequencing

Following quantification on NanoDrop spectrophotometer (Thermo Fisher Scientific), samples were double-checked using Qubit (Invitrogen) and checked on Tapestation 4200 (Agilent Technologies), defining the RNA Integrity Number (RIN). Samples with a RIN ≥ 7 were processed to generate libraries for mRNA sequencing following the Illumina® TruSeq Stranded mRNA Sample Preparation Guide, starting from a defined concentration of 500 ng of material per sample.

Mouse models

Mice were bred in the pathogen-free animal facility of the IRCCS San Raffaele Hospital in accordance with European Union guidelines. The study was approved by the Institutional Animal Care and Use Committee of IRCCS San Raffaele Hospital and the Italian Ministry of Health. Adoptive transfer (AT) of Eμ-TCL1 tumors was performed as previously described [21]. Briefly, 10 × 106 splenocytes from Eμ-TCL1 mice (CD19 + CD5 + leukemic cells > 90%) were transplanted by intravenous injection into 8-week-old C57BL/6N wild-type male mice (Charles River Laboratories International Inc.,) to generate AT-Eμ-TCL1. Transplanted mice were monitored weekly for leukemia development by flow cytometry of PB samples. Four weeks after transplant (10–20% CD19 + CD5 + leukemic cells in PB), mice were randomized to treatment with UVI5008 at 20 mg/kg or 40 mg/kg or vehicle. UVI5008 was dissolved in a solution containing 8% DMSO, 2.5% Tween 80, and 89.5% oil, according to [20] and administered every other day for a total of 8 administrations. At necropsy, CD19 + CD5 + leukemic

cell content in spleen, femoral BM, and PB was assessed by flow cytometry.

See Supplementary Methods for all detailed protocols and experimental conditions.

Results

UVI5008 is a novel non-covalent BTKi able to evade the C481S mutation

UVI5008 was previously reported to be a potent, multi-target epigenetic inhibitor, exhibiting remarkable anti-cancer activity across various cancer models [20]. Building on these findings and through structural evaluation, we focused and investigated the potential kinase inhibitory activity of UVI5008 in kinase-driven cancer contexts. Initially, UVI5008 demonstrated a marked pro-apoptotic effect in CML cell line (K562), associated with significant inhibition of ABL1 kinase activity and accompanied by both reduced phosphorylation of CRKL and downregulation of the anti-apoptotic protein BCL-XL (Figure S1A-E). To explore our hypothesis, we performed a kinase profiling assay against a panel of ~ 490 human kinases using Thermo Fisher's SelectScreen. UVI5008, at 5 µM, selectively inhibited a subset of eight tyrosine and serine/threonine kinases, BTK, FGR, JAK3, PRKCB2 (PKCβII), PRKCD (PKCδ), CHEK2 (CHK2), MAPK8 (JNK1), and TEC, with at least 30% inhibition (Fig. 1A). Particularly, we focused on the inhibitory effect and molecular binding of UVI5008 against BTK due to its well-established role in B-cell malignancies and the urgent need for alternative inhibitors in ibrutinib-resistant patients [22].

We previously reported that UVI5008 undergoes intracellular metabolism, generating two pharmacologically active fragments of the corresponding thiols (UVI5008-half), suggesting its function as a prodrug [20]. The cleavage at the central disulfide bridge, likely yielding smaller and more flexible metabolites that retain biological activity. We therefore performed a comprehensive computational analysis of the binding affinity and interaction profiles between UVI5008 and UVI5008-half with BTK. A series of in silico investigations were conducted, using ibrutinib and pirtobrutinib as negative and positive reference compounds, respectively, in terms of their differential capability to overcome BTK C481S mutation-associated resistance.

Ibrutinib, an irreversible BTKi, forms a covalent bond with the BTK C481 residue by a thial-Michael addiction to the acrylamide unit, a key anchoring point within the active site (Figure S2AF). Its covalent interaction is also stabilized by a hydrogen bond between the hydroxyl group of the ligand in its protonated resonance form. Additional interactions contribute to stabilization of the ibrutinib–BTK complex and its inhibitory activity. Remarkably, Phe540 participates in a π–π stacking

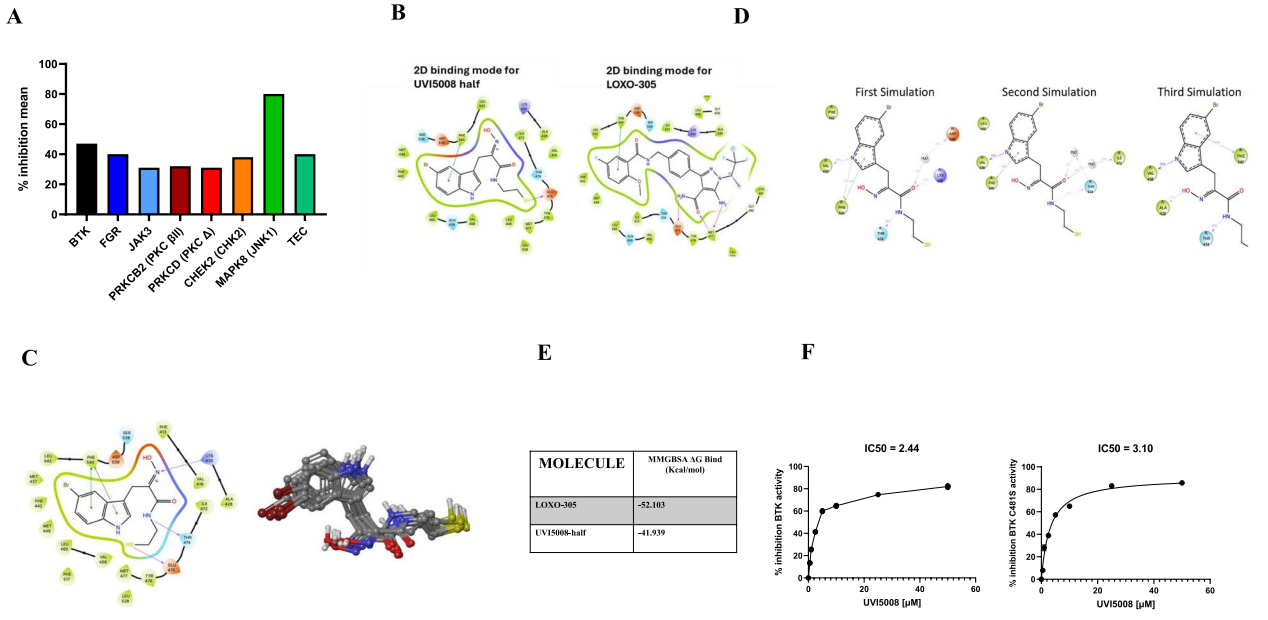

Fig. 1 UVI5008 acts as a novel non-covalent BTKi able to evade the C481S mutation **(A)** Kinase profiling (5 µM, 24 h) identifying selective inhibition of eight kinases: BTK, FGR, JAK3, TEC, PRKCB2, PRKCD, CHEK2, and MAPK8. Data are mean ± SEM; t-test: *p < 0.05, **p < 0.01, ***p < 0.001, ****p < 0.0001. **(B)** Static docking of pirtobrutinib and UVI5008 showing distinct but converging binding modes; H-bonds (purple arrows), π–π interactions (green lines). **(C)** Induced-fit docking (IFD) of UVI5008_half showing consistent binding orientation; key interactions involve residues 474, 475, 540, and Lys430. **(D)** MM-GBSA analysis indicating stable binding of UVI5008_half in its best pose. **(E)** Molecular dynamics simulations confirming stable binding and interaction profile across three replicates. **(F)** BTK kinase assay (WT and C481S) with UVI5008 at increasing concentrations; Data are presented as mean ± SEM, and statistical significance was assessed using a paired t-test (*p < 0.05; **p < 0.01; ***p < 0.001; ****p < 0.0001)

interaction with the terminal aryl ring of the diary ether fragment, contributing to binding affinity. Furthermore, the ibrutinib scaffold participates in a well-defined hydrogen bonding network involving residues such as Glu475 and Met477, which are essential interactions for effective inhibition of BTK's kinase activity (Figure S1B) [23]. Interestingly, from available crystal structures of pirtobrutinib (PDBid8FLL) and computational analysis of UVI5008-half, the two molecules bind the BTK protein in a reversible comparable manner, without engaging in a covalent interaction with Cys481, the critical residue targeted by ibrutinib for irreversible inhibition (Fig. 1B). The binding mode of pirtobrutinib showed critical interactions that are essential for its inhibitory activity. Notably, UVI5008-half accommodates the indole ring into a hydrophobic pocket where Phe540 establishes a π–π stacking interaction with the aromatic portion of the ligand, while Glu475 and Met477 participate in a hydrogen bonding network contributing to the overall binding process and kinase activity inhibition. In the case of UVI5008-half, computational docking and induced-fit docking simulations suggested that it adopts a stable binding pose within the BTK active site, although it showed greater flexibility than pirtobrutinib. This flexibility can be attributed to the smaller molecular size and the presence of a relatively long chain of rotatable bonds. Therefore, the ligand exhibited some variability in its interaction partners during conformational sampling. Nevertheless, the molecule ultimately adopted a converged binding conformation, consistently stabilized by key residues, such as Thr474, Phe540, and Glu475 (Fig. 1C), most of which are also involved in the binding of pirtobrutinib. To further assess the stability of UVI5008-half within the BTK binding pocket, three independent 250 ns MD simulations were performed, each starting from a random seed (Fig. 1D). Throughout all simulations, the binding pose of UVI5008-half remained stable. Notably, residues Phe540 and Thr474 consistently maintained interactions with the ligand, suggesting their critical role in stabilizing the binding conformation. In contrast, the hydrogen bond between the thiol group of UVI5008-half and Glu475, initially observed in static docking models, was not retained during MD trajectories, suggesting that this interaction is likely transient in nature. From a computational analysis of ligand–protein binding energy, pirtobrutinib exhibited a higher binding energy and was also more stable in maintaining its binding pose, although the complex with UVI5008-half was also stable, with a negative ΔG binding of ~ − 42 kcal/mol (Fig. 1E). To assess whether UVI5008 is also effective in inhibiting mutant BTK, we performed kinase assays using both wild-type BTK and the C481S mutant. As shown in Fig. 1F, UVI5008 demonstrated inhibitory activity against the C481S variant, indicating its potential effectiveness in overcoming resistance associated with this clinically relevant mutation. The stability of the UVI5008–BTK interaction was further confirmed by CETSA. Results demonstrated that the binding remained stable up to 85 °C at 5 μM, and 70 °C at 0.5 μM, highlighting the robustness of the interaction across a range of temperatures and suggesting a strong binding affinity even at lower concentrations (Figure S2B). Importantly, CETSA also confirmed that UVI5008 directly engages the active, phosphorylated form of BTK (p-BTK), with a thermal stabilization profile comparable to total BTK (Figure S3A). Together, these results provide compelling evidence that UVI5008 and its metabolite UVI5008-half exert stable interactions with BTK through a non-covalent mechanism that bypasses the C481S resistance-related mutation. The conformational flexibility and stable BTK binding of UVI5008 support its role as a metabolically activated prodrug with strong therapeutic potential able to overcome resistance in relapsed or refractory patients unresponsive to covalent BTKi.

UVI5008 exerts synergistic and enhanced anti-tumor effects in B-cell malignancies through its epigenetic, transcriptional, and enzymatic inhibition of BTK

Given the stable enzymatic inhibition of BTK by UVI5008, we selected appropriate cellular models to assess its anti-tumor effects. These included the Mec-1 CLL cell line and two MCL cell lines, Mino and Granta-519, exhibiting varying degrees of resistance to ibrutinib treatment. UVI5008 treatment at 5 μM for 24 h significantly reduced cell viability and increased apoptotic pre-G1 cells in all three B-cell malignancy lines. (Fig. 2A and B). Notably, these effects were stronger than those exerted by ibrutinib, potentially due to UVI5008's dual mechanism of action combining enzymatic inhibition and epigenetically mediated downregulation of BTK expression, possibly along with collateral modulation of additional kinases. Remarkably, UVI5008 not only reduced BTK phosphorylation and induced efficient disruption of BCR signaling, but also markedly downregulated BTK expression at both mRNA and protein level (Fig. 2C).

To exhaustively assess whether UVI5008 also acts as an epigenetic regulator on the BTK promoter region, we performed chromatin immunoprecipitation (ChIP)-qPCR analysis using Mec-1 cells. Specifically, we investigated key histone modifications associated with transcriptional regulation, including H3K9/14 acetylation (open chromatin) and H3K27 trimethylation (closed chromatin), as well as recruitment of active RNA polymerase II. UVI5008 epigenetically targeted the BTK promoter region, profoundly reshaping chromatin architecture, particularly near the transcription start site (Fig. 2D).

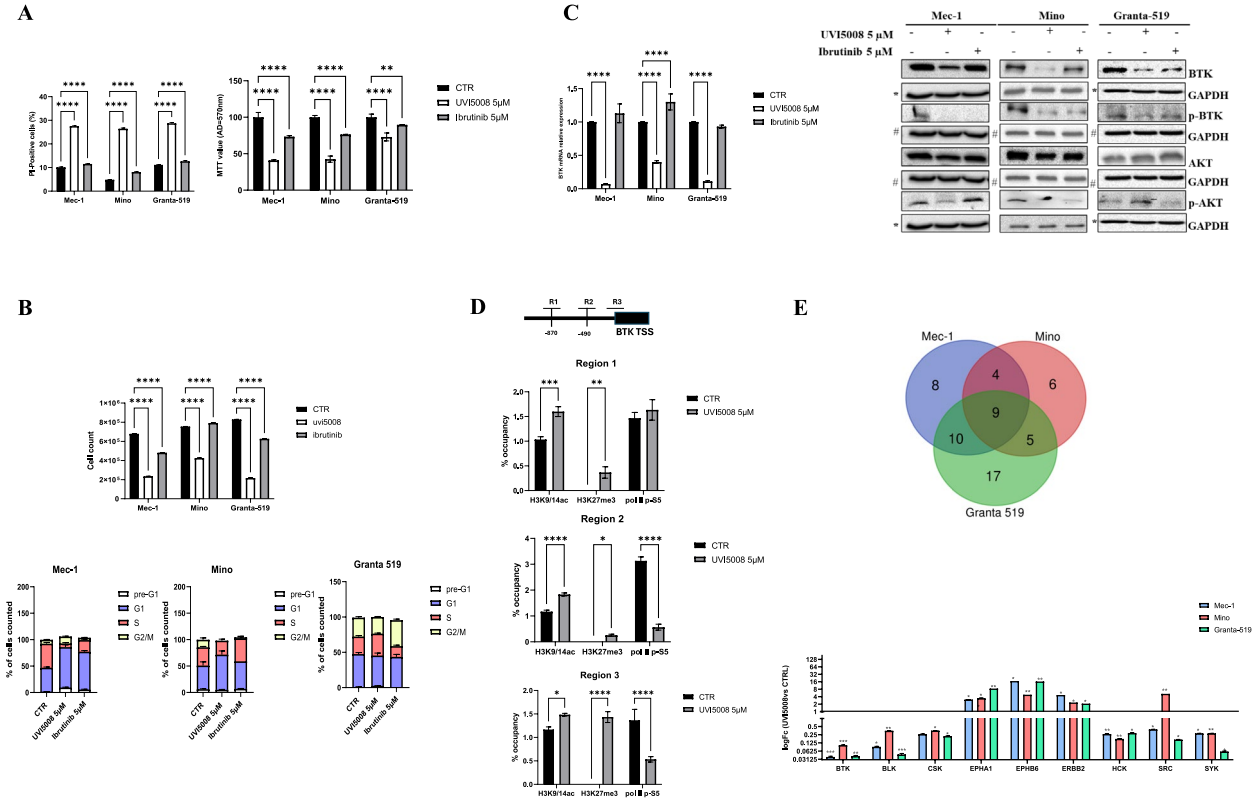

Fig. 2 UVI5008 exhibits BTK inhibitory activity in CLL cells. **(A)** Cytotoxicity of UVI5008 and ibrutinib (5 μM, 24 h) in Mec-1, Mino, and Granta-519 cells assessed by trypan blue (left) and MTT assay (right). **(B)** FACS analysis of cell viability (PI, top) and cell cycle (bottom) after treatment. **(C)** BTK mRNA levels (left) and Western blot of BTK, p-BTK, AKT, and p-AKT (right) after treatment. GAPDH was used for normalization (* and # indicate the same loading control for the corresponding cell line). DMSO was used as the control condition (CTR). **(D)** ChIP-qPCR in Mec-1 cells after UVI5008 (5 μM, 24 h) showing changes in H3K9/14ac, H3K27me3, and p-Ser5 RNA Pol II at BTK promoter**. (E)** Venn diagram (upper) and heatmap (lower) of differentially expressed kinases shared across all three cell lines after UVI5008 treatment. Data are presented as mean ± SEM, and statistical significance was assessed using a paired *t*-test ± SEM; T-test: *p < 0.05, **p < 0.01, ***p < 0.001, ****p < 0.0001

Next, we assessed the potential transcriptional regulation of a panel of 89 tyrosine kinases after 24 h of treatment with UVI5008 at 5 μM, obtaining a list of 31 differentially expressed genes in Mec-1 cells, 24 in Mino cells, and 41 in Granta-519 cells (Supplementary Table 2). Only 9 genes were commonly differentially expressed across all three B-cell malignancy cell lines after UVI5008 treatment: SYK, HCK, EPHA1, SRC, BLK, EPHB6, CSK, ERBB2, and BTK (Fig. 2E). Consistently, UVI5008 significantly downregulated BTK in all tested cell lines, along with SYK and CSK, suggesting a broader inhibition of the BCR signaling pathway.

To further unravel the role of UVI5008, we performed transcriptomic profiling via RNA sequencing (RNA-seq) on Mec-1, Mino, and Granta-519 cell lines following 24 h of treatment with UVI5008. Transcriptional expression profiles revealed that 5590 upregulated and 2442 downregulated genes were shared between all three cell lines after UVI5008 treatment (2 ≤ fold change ≤ − 2; p-value < 0.05) (Figure S2C left panel, and S2D left panel). GO enrichment analysis of the top 10 most enriched biological processes among commonly regulated genes across all cell lines, separated into upregulated and downregulated groups (Figure S2C, right panel, and S2D, right panel), clearly revealed the specificity and cancer system-dependent activity of UVI5008, particularly evident in pathways associated with downregulated genes. UVI5008 treatment led to the consistent downregulation of several immune-related pathways across all tested cell lines, including B-cell activation, immune response, activation and regulation of signaling pathways, lymphocyte and leukocyte activation, activation and positive regulation of immune response, and RNA processing. These pathways are directly linked to BTK-mediated BCR signaling, highlighting the broad impact of UVI5008 on cellular programs essential for B-cell malignancy survival and immune regulation.

Analysis of the shared gene expression profile across all cell lines revealed that the differentially expressed genes (absolute fold change ≥ 2; p-value < 0.05) in UVI5008-treated cells consistently displayed the same directional trend compared to controls, independent of the cellular model (Fig. 3A and B). GSEA for KEGG pathways showed the union of the pathways with highest (n = 4;

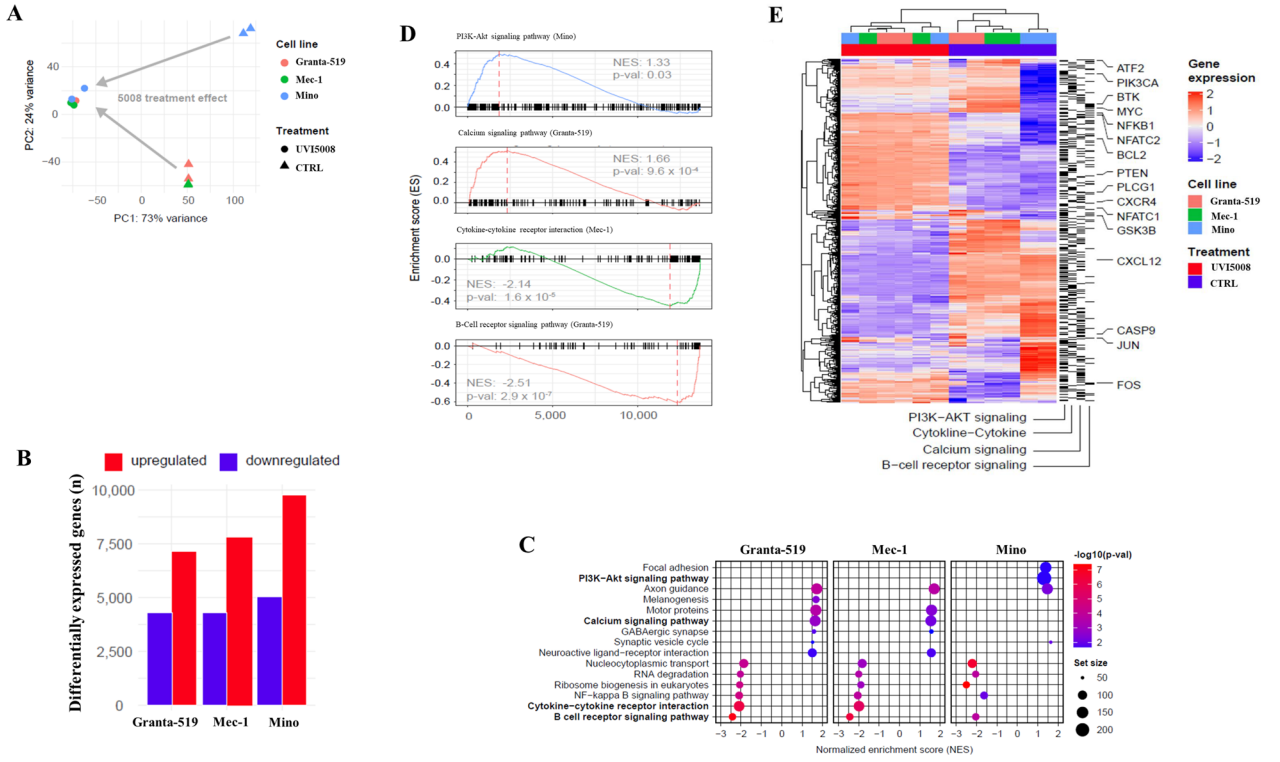

Fig. 3 Transcriptomic analysis of UVI5008-treated CLL cell lines. **(A)** PCA plot based on the 500 most variable genes**. (B)** Number of differentially expressed genes (abs. fold change ≥ 2, p < 0.05) in UVI5008 vs. control. **(C)** GSEA of KEGG pathways: top 4 enriched (upregulated) and bottom 4 suppressed (downregulated) per cell line**. (D)** Running enrichment scores for two up- and two downregulated KEGG pathways. **(E)** Heatmap of genes in pathways from **(F)**; genes with low expression (< 50 reads) were excluded. Color scale indicates log-normalized expression; black ticks mark genes in each pathway. Representative genes are labeled. All p-values were adjusted (Benjamini-Hochberg)

overrepresentation of upregulated genes) and lowest (n = 4; overrepresentation of downregulated genes) normalized enrichment score (NES) per cell line (Fig. 3C and D).

Comprehensive analysis of commonly differentially expressed genes from RNA-seq data revealed the modulation of four key pathways following UVI5008 treatment: BCR signaling and PI3K-AKT signaling, thus confirming previous findings, as well as cytokine–cytokine receptor interaction and calcium signaling. In Fig. 3E, the gene expression heatmap of differentially expressed genes involved in pathways shown in Fig. 3D highlights that UVI5008 impacts BTK, the immune microenvironment, and intracellular signaling, key elements in B-cell malignancies, which may contribute to its therapeutic efficacy through alteration of immune responses and cellular mechanisms driving tumor progression. Together, these findings indicate that UVI5008 is a potent dual-action agent that combines enzymatic inhibition and epigenetic repression of BTK effectively disrupting key survival pathways in B-cell malignancies.

Preclinical evaluation of UVI5008 in ex vivo patient-derived CLL cells

Our study included ex vivo analysis of primary patient-derived cells from a cohort of 52 CLL patients (Supplementary Table 1). All samples were collected from peripheral blood and processed to assess both the presence of BTK mutations, with no genetic aberrations detected at the time of analysis (data not shown), and their responsiveness to UVI5008 treatment. UVI5008 treatment significantly increased cell death in CLL patient-derived samples, compared to ibrutinib, as assessed by PI-positivity using flow cytometry (Fig. 4A). Based on treatment responsiveness, samples were stratified into two subgroups. We defined a fold change threshold for cell death (CD) induction, categorizing patients as either Responsive (R) (fold change CD ≥ 2) or Non-Responsive (NR) (fold change CD < 2). The results indicate a stronger and more rapid response to UVI5008 compared to ibrutinib. Specifically, the percentage of UVI5008-responsive samples reached 38% at 24 h and 66% at 48 h, in contrast to the lower and stable responsiveness observed with ibrutinib, which remained within the 14–18% range over the same time points (Fig. 4B).

We also investigated the impact of UVI5008 on cell cycle dynamics and observed a marked accumulation of

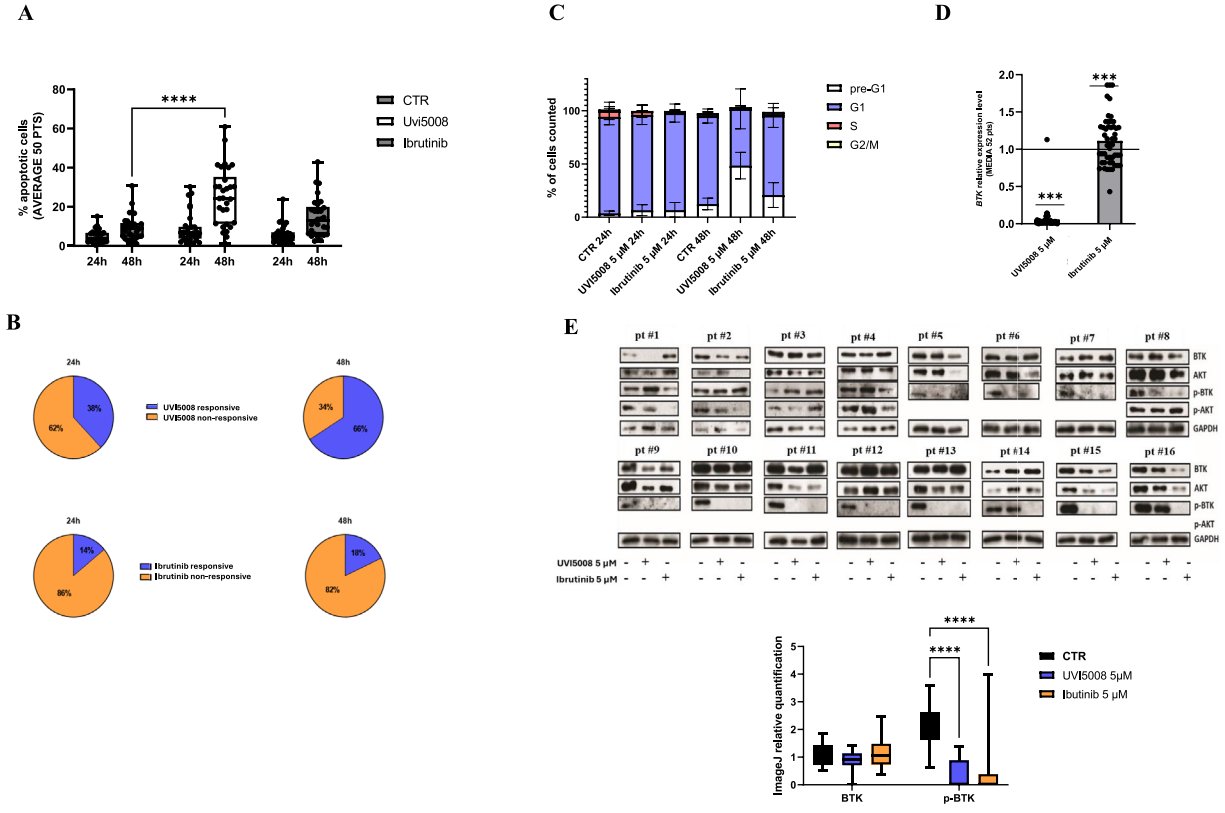

Fig. 4 UVI5008 effects in CLL patient samples and Eμ-TCL1 mouse model. **(A)** PI cell viability staining of Mec-1, Mino, and Granta-519 cells after 24 h treatment with UVI5008 or ibrutinib (5 μM). **(B)** Pie chart showing patient stratification by treatment response (≥ twofold increase in cell death). **(C)** Cell cycle analysis by FACS after 24 h treatment with UVI5008 or ibrutinib (5 μM). **(D)** BTK mRNA (median of 50 CLL patients, left) and Western blot of BTK, p-BTK, AKT, and p-AKT (right) following 24 h treatment with UVI5008 or ibrutinib (5 μM). **(E)** WB on analysis on a cohort of 16 patients to assess BTK, AKT, pBTK, and pAKT expression after 24 h treatment with UVI5008 or ibrutinib (5 μM). DMSO was used as the control condition (CTR). Data are presented as mean ± SEM, and statistical significance was assessed using a paired *t*-test *p < 0.05, **p < 0.01, ***p < 0.001, ****p < 0.0001

cells in pre-G1 phase following treatment, which resulted in only 20% accumulation under the same conditions (Fig. 4C). The molecular effects of UVI5008 on BTK expression led to a dramatic reduction in BTK mRNA (Fig. 4D). Additionally, we observed a negative regulation of BTK and its downstream protein targets at protein level in almost all tested CLL patient-derived samples (n = 16) (Fig. 4E, left right panel, representative group), further supporting the impact of the compound on BTK signaling. Together, these results demonstrate that UVI5008 exerts potent antileukemic effects in primary CLL samples, as observed in cell lines, showing superior efficacy compared to ibrutinib by effectively inducing cell death, disrupting cell cycle progression, downregulating BTK expression at transcriptional and protein level, and inhibiting BTK enzymatic activity.

Preclinical evidence of UVI5008 in Eμ-TCL1 mouse models

To explore the potential therapeutic value of UVI5008 in CLL, we utilized the Eμ-TCL1 syngeneic tumor transfer (AT) CLL murine model. C57BL/6 wild-type recipient mice received 10×10^6 splenocytes derived from donor Eμ-TCL1. When AT-Eμ-TCL1 mice reached a disease range between 10 and 20% of malignant cells ($CD19^+CD5^+$) in PB, they were randomized into four groups to receive intraperitoneally UVI5008 at either 20 mg/kg (n = 4) or 40 mg/kg (n = 4) or vehicle (n = 4) every second day, or to remain untreated (n = 4). Mice were sacrificed after 8 doses of treatment to evaluate disease expansion in PB and lymphoid tissues (Fig. 5A). Mice treated with UVI5008 at 20 mg/kg displayed a decreasing trend in the number of leukemic cells in lymphoid tissues compared to control vehicle-treated mice. More importantly, the higher UVI5008 dosage (40 mg/kg) promoted a decrease in spleen size and weight (Fig. 5B) and a statistically significant reduction in leukemic cells in spleen, BM, and PB compared to controls (Fig. 5C). In addition, BTK and p-BTK expression were evaluated in experimental mouse groups treated with UVI5008 at 20 mg/kg and 40 mg/kg, compared to vehicle-treated and untreated controls. UVI5008 administration induced a dramatic reduction in BTK mRNA levels, accompanied by a pronounced decrease in both total BTK and its active, phosphorylated form (Figure S3B).

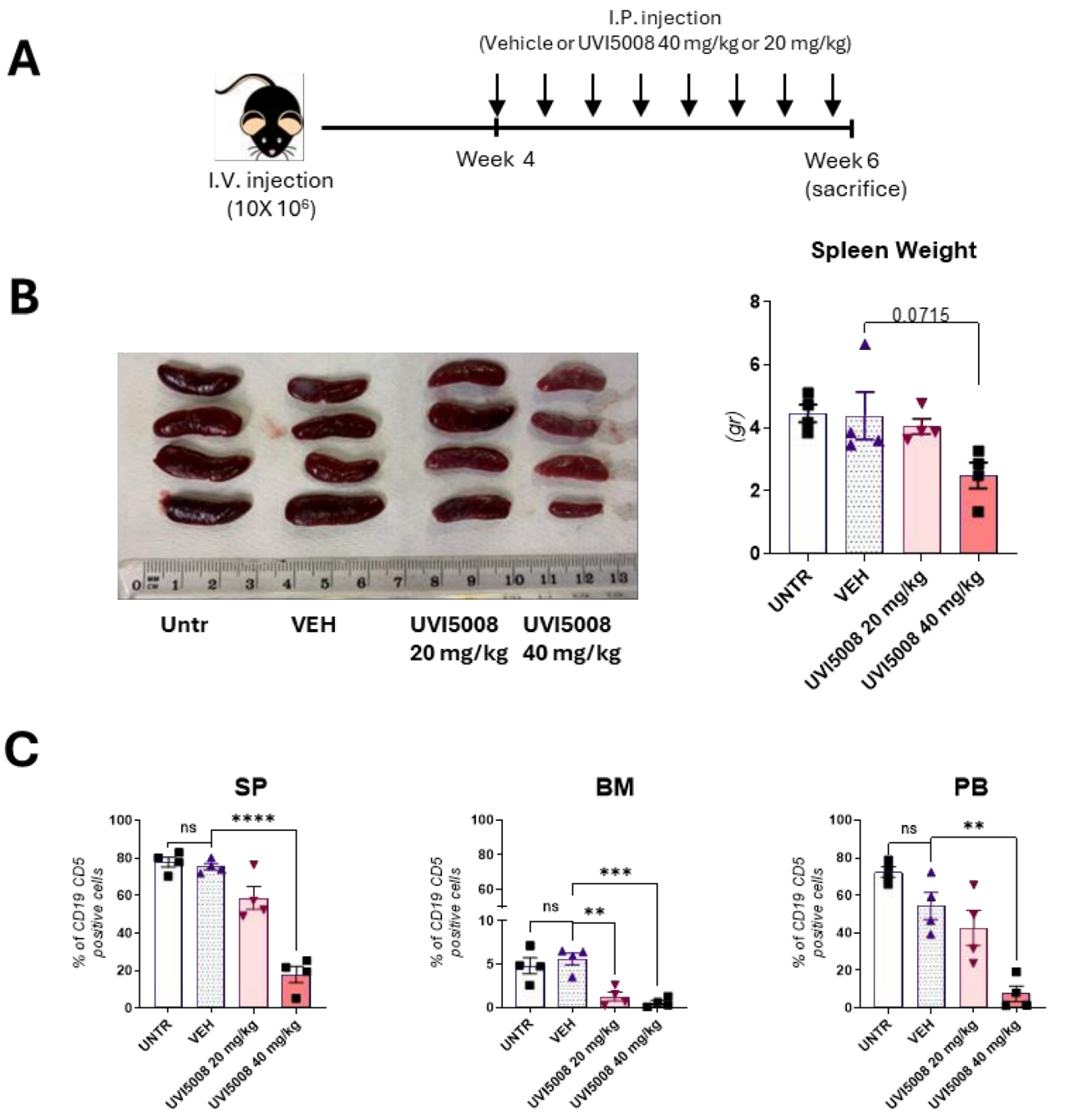

Fig. 5 UVI5008 treatment reduces disease development in the AT-Eμ-TCL1 CLL model. **(A)** Experimental scheme. Four weeks after transplant (10–20% CD19 + CD5 + leukemic cells in PB), mice were randomized to treatment with UVI5008 at 20 mg/kg or 40 mg/kg or vehicle; administered every other day for a total of 8 administrations. **(B)** Image (left) and weight (right) of spleens explanted from AT-Eμ-TCL1 mice at sacrifice after 8 doses of UVI5008 or vehicle or left untreated (UNTR). **(C)** Number of $CD19^+$ and $CD5^+$ leukemic cells measured in spleen, bone marrow, and peripheral blood of mice by flow cytometry. Values are mean ± SEM. Statistical differences were assessed by one-way ANOVA followed by Dunnet's multiple comparison test (** $p < 0.01$, *** $p < 0.001$, **** $p < 0.0001$)

Within the available spleen flow cytometry datasets from the TCL1 model, we assessed the impact of UVI5008 on non-malignant $CD19^+CD5^-$ B cells and $CD19^-CD5^+$ populations. UVI5008 spared these non-malignant populations, which showed a slight increase (Figure S4). As expected, mice treated with UVI5008, or vehicle alone developed peritoneal ascites caused by the chemical composition of the vehicle. These findings demonstrate that UVI5008 effectively suppresses CLL progression in vivo in a dose-dependent manner, significantly reducing leukemic burden across key tissues.

Discussion

This study identified a new therapeutic application for UVI5008, a known anticancer epi-drug, as a non-covalent epigenetic inhibitor of BTK, underscoring its potential in BCR-driven malignancies. Our findings position UVI5008 as a promising alternative or addition to current BTK-targeted therapies. Based on initial insights into the potential collateral activity of UVI5008, we expanded our investigation, hypothesizing, and ultimately discovering its new activity as a kinase inhibitor.

The therapeutic value of UVI5008 lies in its ability to inhibit BTK through two distinct mechanisms: epigenetically, by repressing its transcription through promoter closure, and directly, by binding to and inhibiting the BTK enzyme. This dual mechanism represents the true novelty of the drug, which enhances its therapeutic efficacy against BTK as well as the BTK C481S mutant and establishes UVI5008 as a groundbreaking alternative to conventional BTKi. Initially, we observed that UVI5008 inhibited ABL1 and exhibited anticancer effects in CML. A kinase profiling assay against 490 human kinases revealed that UVI5008 selectively inhibits a subset of eight tyrosine and serine/threonine kinases, including BTK, FGR, JAK3, PRKCB2, PRKCD, CHEK2, MAPK8, and TEC, with at least 30% inhibition. This suggests that the compound has a non-promiscuous pharmacological profile, minimizing the risk of off-target effects. Given the significant role of BTK in B-cell malignancies and the clinical need for alternative BTKi in ibrutinib-resistant patients, this work focused on BTK as the primary target. Interestingly, ABL1 inhibitors such as dasatinib also show BTK inhibitory activity, strengthening the rationale for investigating UVI5008 in BTK-dependent B-cell malignancies.

In silico studies using ibrutinib and pirtobrutinib as reference compounds corroborated and strengthened a stable interaction between UVI5008 and BTK. UVI5008 undergoes intracellular metabolism, generating active fragments including UVI5008-half. MD simulations suggested that UVI5008-half binds stably to BTK without engaging in a covalent interaction with Cys481, the target residue of ibrutinib. UVI5008-half was stable in its binding pose, with key interactions at Thr474 and Phe540. Binding energy computational analysis revealed that UVI5008-half exhibits a negative ΔG of binding ~ −42 kcal/mol (MMGBSA), indicating a stable interaction with BTK, a finding further confirmed by CETSA, which demonstrated robust thermal stabilization of the UVI5008–BTK complex up to 85 °C at 5 μM, and 70 °C at 0.5 μM. To strengthen our binding mode hypothesis, in silico covalent docking approaches were set to evaluate if a covalent binding was possible, firstly considering known reactive moieties within the UVI5008-half molecule [24, 25]. For Michael addiction, nucleophilic substitution or nucleophilic addition, no energetically favorable solutions were retrieved analyzing Cys481 and other possible reactive residues surrounding the ligand. Moreover, considering the stable binding pose proposed by in silico analysis, the Bromine substituted indole seems to accommodate into a hydrophobic pocket, where there are no reactive residues, in proximity, that could interact through a possible SN2 nucleophilic substitution with Br. Indeed, these preliminary evaluations suggest a non-covalent binding mechanism.

UVI5008 appears able to overcome resistance in patients harboring the BTK C481S mutation. Notably, its inhibitory activity against the mutant BTK makes it comparable to pirtobrutinib, the most advanced next-generation BTKi already FDA/EMA-approved for treatment of CLL (72% overall response rate in relapsed or refractory patients). In this context, the comparable inhibitory activity, binding stability, and non-covalent interaction profile of UVI5008 against the BTK C481S mutant position the compound as a highly promising therapeutic alternative. Additionally, UVI5008 metabolism offers a significant advantage as a potential prodrug. The active metabolite, UVI5008-half, retains its biological activity, suggesting that lower effective doses may be sufficient to achieve therapeutic effects, potentially reducing toxicity and enhancing tolerability.

Using established cellular models of CLL (Mec-1) and MCL (Mino, Granta-519), we confirmed that UVI5008 significantly reduces viability, and induces apoptosis, particularly after 48 h. Mechanistically, UVI5008 not only inhibits BTK phosphorylation and disrupts BCR signaling, as ibrutinib does, but also reduces BTK expression at both mRNA and protein level. This dual effect on BTK suggests that UVI5008 may overcome resistance linked to persistent BTK expression despite kinase inhibition. Importantly, our ChIP-qPCR data show that UVI5008 induces epigenetic remodeling at the BTK promoter, characterized by reduced H3K9/14 acetylation, increased H3K27 trimethylation, and diminished active RNA polymerase II recruitment. These findings indicate that UVI5008 not only targets BTK functionally but also transcriptionally, by promoting a repressive chromatin state that silences its gene expression.

Transcriptome-wide RNA-seq analysis further underscored the wide-ranging effects of UVI5008. Thousands of genes were commonly modulated across all three cell lines, with a strong convergence on immune-related biological processes. GO enrichment analysis revealed consistent downregulation of pathways involved in B-cell activation, immune response modulation, lymphocyte activation, and RNA processing. These processes are critically dependent on intact BTK signaling and are central to the survival and function of malignant B-cells. Notably, GSEA confirmed downregulation of key oncogenic

pathways including BCR and PI3K-AKT signaling and revealed alterations in cytokine–cytokine receptor interaction and calcium signaling, suggesting that UVI5008 exerts a comprehensive impact on intracellular and microenvironmental signaling networks. We corroborated our findings by performing ex vivo experiments in primary PB samples from 52 CLL patients. UVI5008 induced significant cell death in patient-derived CLL cells, demonstrating a higher and faster response rate compared to ibrutinib (38% at 24 h and 66% at 48 h vs. 14–18% for ibrutinib). In ex vivo experiments, we observed a robust pre-G1 accumulation, accompanied by a dramatic abrogation of BTK expression and modulation of downstream signaling pathways. In vivo, the Eμ-TCL1 murine model faithfully recapitulated UVI5008-mediated BTK modulation and enzymatic inhibition, demonstrating robust, dose-dependent antileukemic efficacy, with pronounced reductions in spleen size and in selective leukemic cell burden across multiple tissues, while sparing normal hematopoietic populations.

Conclusion

This study unveils UVI5008 as a groundbreaking, first-in-class, non-covalent BTK "epi-inhibitor" and as a novel therapeutic option for CLL. This epi-drug induces rapid, potent cell death in B-cell malignancies through a unique dual action: inhibiting BTK enzymatic activity and silencing its expression via chromatin closure, including in resistant mutants. Further investigation is needed to fully understand its long-term epigenetic effects and potential off-target impacts. Nonetheless, the uniqueness of UVI5008 positions it as an innovative therapeutic opportunity in BTK-dependent malignant B-cell cancers.

Abbreviations

BCR	B-cell receptor
BM	Bone marrow
BTK	Bruton's tyrosine kinase
BTKi	BTK inhibitors
CD	Cell death
CLL	Chronic lymphocytic leukemia
MCL	Mantle cell lymphoma
PB	Peripheral blood
SLL	Small lymphocytic lymphoma

Supplementary Information

The online version contains supplementary material available at https://doi.org/10.1186/s13045-026-01784-9.

Supplementary material 1.

Supplementary material 2: Table 1. Clinical characteristics of chronic lymphocytic leukemia patients. UT (Untreated); FCR (cyclophosphamide-fludarabine-rituximab); R-CHOP (rituximab, cyclophosphamide, doxorubicin, vincristine, and prednisone); R-BENDA (rituximab-bendamustine).

Supplementary material 3.

Supplementary material 4: Table 2. List of differentially expressed kinase genes after 24 hours of treatment with UVI5008 (5 μM). A total of 31 genes were identified in MEC-1 cells, 24 genes in MINO cells, and 41 genes in GRANTA-519 cells. |FC|±2 and $p \leq 0.05$.

Supplementary material 5: Table 3. Alignment and differential analysis of RNA-seq libraries. GO BP and KEGG pathways of downregulated and upregulated genes.

Acknowledgements

Special thanks to Catherine Fisher for language editing.

Author contributions

CD and GS performed the majority of the experiments and wrote the manuscript. CM, and FS performed some of the molecular and cell-based experiments. MC carried out RNA-seq experiments and contributed to data acquisition. WLM was responsible for processing, analyzing, and visualizing RNA-seq results. VC performed some flow cytometry-based analyses. AC, MF, JB, and PPG contributed to the experimental design and analysis of results of in vivo experiments in Eμ-TCL1 mice. RA and ADL provided the compound. DN, FC and VBP contributed to patient recruitment and clinical data collection. WGW and FPT contributed to the implementation of the research. LA and CD contributed to funding acquisition, project conceptualization and supervision, data interpretation, and manuscript preparation, including writing, revision, and editing. All authors reviewed the manuscript.

Funding

This work was supported by FISR2019_00374 MeDyCa, B84G19000200008 (CD); MIMIT-EPI-GA F/350261/01–04/X60, B69I23003210007 (CD); PRIN-2022-PNRR-*SOLAR*-P2022NFCPM, B53D23025100001 (CD); PNRR-PRIN-PNRR-2022 Amoebo-switch P2022F3YRF, B53D23031620001 (LA); MIMIT–NABUCCO F/260018/03/X51, B29J24001270005 (LA); Epi-MET D.M. 31.12.2021, D.D. 18.03.2022 no. 34; Project F/310034/03/X56, B29J24000550005 (LA); DARIA, B73C22001250006 (LA). GS was supported by a post-doctoral fellowship received from PNRR – Missione 4 – Componente 2, NextGeneration EU "MEDUSA", B83C2200068007.

Data availability

Raw and processed RNA-sequencing are available from the Gene Expression Omnibus (GEO) with accession number GSE295723.

Declarations

Competing interests

The authors declare no competing interests.

Disclosure

C. Dell'Aversana and L. Altucci are inventors for the patent no. 102025000013429 entitled: "NUOVO INIBITORE DELLA TIROSIN-CHINASI DI BRUTON, SUOI DERIVATI ED USI FARMACEUTICI"

Author details

[1]Department of Precision Medicine, University of Campania "Luigi Vanvitelli", Naples, Italy
[2]Department of Medicine and Surgery, LUM University, Casamassima, Italy
[3]Institute of Endotypes in Oncology, Metabolism and Immunology "Gaetano Salvatore" (IEOMI), National Research Council (CNR), Naples, Italy
[4]Molecular Informatics Unit, Ri.MED Foundation, Palermo, Italy
[5]Epigenetic Editing, Department of Pathology and Medical Biology, University of Groningen, University Medical Center Groningen, Groningen, The Netherlands
[6]Comprehensive Cancer Center, IRCCS San Raffaele Hospital, Milan, Italy
[7]Medical School, Vita-Salute San Raffaele University, Milan, Italy
[8]Hematology Unit, "Andrea Tortora" Hospital, Pagani, Italy
[9]Department of Organic Chemistry, CINBIO, University of Vigo, Vigo, Spain
[10]Department of Oncology and Hematology, Hematology Unit, "Federico II" University Hospital, Naples, Italy
[11]Stem Cell Transplantation and Cell Therapy Unit, AORN Santobono Pausilipon, Naples, Italy
[12]Department of Leukemia, The University of Texas MD Anderson Cancer Center, Houston, USA
[13]Biogem Institute of Molecular and Genetic Biology, Ariano Irpino, Italy
[14]Medical Epigenetics Program, "Luigi Vanvitelli" Hospital, Naples, Italy

Received: 27 October 2025 / Accepted: 17 February 2026
Published online: 22 February 2026

References

1. Mehra S, Nicholls M, Taylor J. The evolving role of Bruton's tyrosine kinase inhibitors in B cell lymphomas. Int J Mol Sci. 2024. https://doi.org/10.3390/ijms25147516.
2. Uckun FM, Venkatachalam T. Targeting solid tumors with BTK inhibitors. Front Cell Dev Biol. 2021;9:650414.
3. Chen S, Liu Y, Zhang Y, Guo X, Bai T, He K, et al. Bruton's tyrosine kinase inhibition suppresses pathological retinal angiogenesis. Br J Pharmacol. 2024. https://doi.org/10.1111/bph.17344.
4. von Roemeling C, Ferreri AJM, Soussain C, Tun HW, Grommes C. Targets and treatments in primary CNS lymphoma. Leuk Lymphoma. 2024;65(8):1055–67.
5. Eyre TA, Cheah CY, Wang ML. Therapeutic options for relapsed/refractory mantle cell lymphoma. Blood. 2022;139(5):666–77.
6. Mukkamalla SKR, Taneja A, Malipeddi D, Master SR. Chronic Lymphocytic Leukemia. StatPearls. Treasure Island (FL).2025.
7. Aw A, Brown JR. Current status of Bruton's tyrosine kinase inhibitor development and use in B-cell malignancies. Drugs Aging. 2017;34(7):509–27.
8. Jain N, Wierda WG, O'Brien S. Chronic lymphocytic leukaemia. Lancet. 2024;404(10453):694–706.
9. Burger JA, Landau DA, Taylor-Weiner A, Bozic I, Zhang H, Sarosiek K, et al. Clonal evolution in patients with chronic lymphocytic leukaemia developing resistance to BTK inhibition. Nat Commun. 2016;7:11589.
10. Kwok M, Wu CJ. Clonal evolution of high-risk chronic lymphocytic leukemia: a contemporary perspective. Front Oncol. 2021;11:790004.
11. Molica S, Allsup D. Bruton's tyrosine kinase (BTK) mutations in chronic lymphocytic leukemia (CLL): a clinical view. Mediterr J Hematol Infect Dis. 2025;17(1):e2025053.
12. Ibrahim S, Pham N, Sahni A, Sekeres S, Cool A, Taylor J, et al. Pirtobrutinib in the treatment of chronic lymphocytic leukemia or small lymphocytic lymphoma. Future Oncol. 2025. https://doi.org/10.1080/14796694.2025.2567834.
13. Blombery P, Chatzikonstantinou T, Gerousi M, Rosenquist R, Gaidano G, Pospisilova S, et al. Resistance to targeted therapies in chronic lymphocytic leukemia: current status and perspectives for clinical and diagnostic practice. Leukemia. 2025;39(9):2049–60.
14. Baylin SB, Jones PA. A decade of exploring the cancer epigenome - biological and translational implications. Nat Rev Cancer. 2011;11(10):726–34.
15. Zhang X, Wang H, Zhang Y, Wang X. Advances in epigenetic alterations of chronic lymphocytic leukemia: from pathogenesis to treatment. Clin Exp Med. 2024;24(1):54.
16. Esteller M, Dawson MA, Kadoch C, Rassool FV, Jones PA, Baylin SB. The epigenetic hallmarks of cancer. Cancer Discov. 2024;14(10):1783–809.
17. Maietta I, Martinez-Perez A, Alvarez R, De Lera AR, Gonzalez-Fernandez A, Simon-Vazquez R. Synergistic antitumoral effect of epigenetic inhibitors and gemcitabine in pancreatic cancer cells. Pharmaceuticals (Basel). 2022. https://doi.org/10.3390/ph15070824.
18. Conte M, Fontana E, Nebbioso A, Altucci L. Marine-derived secondary metabolites as promising epigenetic bio-compounds for anticancer therapy. Mar Drugs. 2020. https://doi.org/10.3390/md19010015.
19. Zhang Z, Wang G, Li Y, Lei D, Xiang J, Ouyang L, et al. Recent progress in DNA methyltransferase inhibitors as anticancer agents. Front Pharmacol. 2022;13:1072651.
20. Nebbioso A, Pereira R, Khanwalkar H, Matarese F, Garcia-Rodriguez J, Miceli M, et al. Death receptor pathway activation and increase of ROS production by the triple epigenetic inhibitor UVI5008. Mol Cancer Ther. 2011;10(12):2394–404.
21. McClanahan F, Hanna B, Miller S, Clear AJ, Lichter P, Gribben JG, et al. PD-L1 checkpoint blockade prevents immune dysfunction and leukemia development in a mouse model of chronic lymphocytic leukemia. Blood. 2015;126(2):203–11.
22. Bravo-Gonzalez A, Alasfour M, Soong D, Noy J, Pongas G. Advances in targeted therapy: addressing resistance to BTK inhibition in B-cell lymphoid malignancies. Cancers (Basel). 2024. https://doi.org/10.3390/cancers16203434.
23. Voice AT, Tresadern G, Twidale RM, van Vlijmen H, Mulholland AJ. Mechanism of covalent binding of ibrutinib to Bruton's tyrosine kinase revealed by QM/MM calculations. Chem Sci. 2021;12(15):5511–6.
24. Hillebrand L, Liang XJ, Serafim RAM, Gehringer M. Emerging and re-emerging warheads for targeted covalent inhibitors: an update. J Med Chem. 2024;67(10):7668–758.
25. Zheng L, Li Y, Wu D, Xiao H, Zheng S, Wang G, Sun Q. Development of covalent inhibitors: Principle, design, and application in cancer. MedComm–Oncology. 2023.

Publisher's Note